Published in final edited form as:

Magn Reson Imaging Clin N Am. 2021 August ; 29(3): 305–320. doi:10.1016/j.mric.2021.05.002.

CT Techniques, Protocols, Advancements and Future Directions in Liver Diseases

Naveen Kulkarni[1], **Alice Fung**[3], **Avinash R. Kambadakone**[2], **Benjamin M. Yeh**[4]

[1]Department of Radiology Medical College of Wisconsin

[2]Department of Radiology, Oregon Health & Science University

[3]Department of Radiology, MGH

[4]Department of Radiology and Biomedical Imaging, UCSF Medical Center, San Francisco, CA

Abstract

Computed tomography (CT) is often performed as the initial imaging study for the workup of patients with known or suspected liver disease. Our article reviews liver CT techniques and protocols in clinical practice along with updates on relevant CT advances, including wide-detector CT, radiation dose optimization, and multi-energy scanning, that have already shown clinical impact. Particular emphasis is placed on optimizing the late arterial phase of enhancement, which is critical to the evaluation of hepatocellular carcinoma (HCC). We also discuss emerging techniques that may soon influence clinical care.

Keywords

Liver; CT; CT Technique; Late Arterial Phase; Dual Energy CT

Introduction

CT is often chosen for the initial workup of focal and diffuse liver disease because it is well tolerated, the images have few artifacts, and the entire abdomen and pelvis can be imaged quickly within a single breathhold (1). In the past decade, CT technology has advanced rapidly such that most modern scanners have the capability to image with wide detector arrays, low kilovoltage (kVp) settings, iterative reconstruction, dual energy CT (DECT) and now deep learning image reconstructions (2). Attention to imaging parameters is now more important than ever for optimal evaluation of liver disease.

Corresponding author: Benjamin Yeh, MD, Department of Radiology and Biomedical Imaging, University of California San Francisco, 505, Parnassus Ave, San Francisco, CA 94143-0628, Tel: 415-514-9318, Benjamin.Yeh@ucsf.edu.

General technique considerations

Hardware

Multi-detector row CT (MDCT) has become the norm such that modern CT scanners typically have 4–64 detector rows that allow large Z-axis coverage in a single rotation with isotropic resolution (down to 0.5-mm)(3). Premium CT scanners offer even wider detectors with up to 320 detector rows that cover up to 16 cm in the z-axis and fast gantry rotation times down to 0.25sec(3). Such scanners include the Revolution Apex, General Electric Healthcare; the Force, Siemens; and Aquilion ONE Vision, Canon. Scanning in the axial mode eliminates artifacts that are associated with the helical scanning technique(4), but should be performed with caution in the liver so as to not exclude portions of the organ.

CT systems with wide-detector configuration are at disadvantage from increased scatter, heel effect, cone-beam artifacts, and the trade-off between spatial resolution and image noise due to the large cone angle that may impact low contrast resolution. To compensate for such negative effects on image quality, some CT manufacturers have introduced advanced 3-D anti-scatter grids(5). Although wide-detector systems have shown encouraging results in cardiovascular applications, it's value in other applications such as liver imaging needs to be established.

Scan times of less than one second can minimize motion in patients who are not cooperative or unable to breathhold and decrease radiation exposure(3, 4). Wide-detector CT systems permit protocols to image the entire liver (in axial mode) at multiple time points during the early/late arterial phase which may potentially detect more hypervascular liver lesions than single arterial phase scans(6). Wide-detector scanners also allow whole-liver dynamic perfusion imaging which is not feasible on CT systems with limited Z-axis coverage(7).

Radiation dose considerations

The need to limit radiation dose at CT to as low as reasonably allowable (ALARA) is universally recognized, particularly for multi-phase exams which are required for most dedicated liver scans(8). Despite the need to limit radiation exposure, an essential guiding principle is that CT images must be diagnostic to be useful(5). Radiation dose tracking software is used at many institutions to flag CT scans that are obtained with unexpectedly high doses. Generally these scans are obtained in morbidly obese patients and are justified, but monitoring helps reduce inadvertent over-radiation and allows for follow-up of affected patients.

Radiation dose is proportional to the tube current (mA). Modern CT scanners allow for automatic tube current modulation (ATCM) along the Z-axis based on patient density on the scout image to achieve a target acceptable noise level(9). Use of ATCM may reduce radiation dose by up to 50% compared with fixed mA(10).

Radiation dose is exponentially reduced at lower kVp settings(11). When the tube current is held constant, lowering the tube potential from 120 to 100 kVp or 120 to 80 kVp may reduce dose by 33% and 65%, respectively (12, 13). Reduced kVp settings also increase the attenuation of iodine contrast by up to 70% (Figure 1). Although the low kVp technique

can be applied in thinner adults while maintaining acceptable image noise, its application to large patients is commonly limited due to noise, owing to excessive attenuation of low energy X-rays by thick body parts(14). In fact, for severely obese patients, high kVp settings (140 or 150 kVp) are frequently needed to achieve sufficient X-ray penetration for diagnostic scans. New CT systems with high output X-ray tubes partially overcome the X-ray attenuation concerns of lower kVp, and automated kVp selection may assist in choosing appropriate kVps for patients of different sizes(12, 15).

Powerful X-ray tubes have also been developed that help exploit the benefits of low kVp technique in patients across different body habitus, including large patients, with some high-end tubes capable of providing tube current up to 1800mA even at 70/80kVp settings(3). Although one may perceive that higher tube power means a higher dose to the patient, high tube power allows for using a stronger prefiltration by using dedicated prefilters to remove excessively low energy photons from the beam that would contribute disproportionately to the patient dose but not to image quality(15).

Iterative reconstruction has further enabled radiation dose reduction by reducing CT image noise. In conjunction with other approaches, iterative reconstructions has enabled radiation dose reduction of up to 75% while maintaining acceptable image noise and quality (Figure 1). However, one should be cautious with aggressive radiation dose reduction as several recent studies have demonstrated that low contrast lesion detection is not maintained at moderate to large levels of dose reduction and can limit the detection and characterization of hypodense hepatic lesions such as liver metastases, particularly for sub-centimeter lesions(13, 16, 17).

Liver CT technique

Although CT is generally considered to be non-operator dependent and robust, careful attention to imaging technique remains crucial for optimal detection and characterization of liver pathologies. Table 1 describes general CT and contrast parameters for multiphase liver CT.

Unlike for angiographic imaging which can be obtained with small doses of accurately timed contrast material to opacify the arteries, optimal liver imaging generally requires robust contrast enhancement of the entire hepatic vasculature (artery, portal vein, and hepatic veins) and liver parenchyma which can only be consistently acquired by the rapid injection of relatively large doses of intravenous (IV) contrast material. Use of adequately large IV contrast doses is particularly important for multiphase imaging for the detection and characterization of liver lesions including metastases and hepatocellular carcinoma (HCC). It is valuable to use the same kVp setting for all phases of a liver exam so that HU values are directly comparable between phases.

Noncontrast Phase

The noncontrast (precontrast) phase serves as a baseline for determining the extent of liver lesion enhancement with IV contrast and is useful to assess background liver disease such as steatosis. For certain tumors such as neuoroendocrine metastases, the noncontrast CT is

often the best phase by which to compare scan-to-scan tumor size. For HCC evaluation, the precontrast phase helps identify subtle areas of arterial phase hyperenhancement (18, 19). Some institutions use lower radiation dose for the noncontrast phase compared to the postcontrast phases. If the patient has undergone locoregional treatment, the precontrast phase is valuable to distinguish iodized oil staining, blood, and proteinaceous material from true arterial phase hyperenhancement (20). Nevertheless, controversy exists for its use in assessing focal liver lesions. For CT imaging of treatment-naïve HCC, the inclusion of a noncontrast phase is optional by LI-RADS and other HCC staging standards.

Post-Contrast Phases

Intravenous contrast plays a critical role in the detection and characterization of focal liver lesions. While the portal venous phase is sufficient for the detection of hypovascular liver metastases, the late arterial and delayed phases are most important for the evaluation of hypervascular tumors including HCC. Multiple factors govern the quality of a multiphase liver CT (21). While portal venous phase parenchymal enhancement is mainly related to iodine dose as delineated by contrast medium volume and iodine concentration, the quality of late arterial images depends on rapid contrast injection and accurate scan timing (22).

Late Arterial Phase

Achieving an optimal late arterial phase scan is critical for the detection of hypervascular liver lesions, such as HCC. The late arterial phase shows hypervascular lesions against a minimally enhanced liver parenchyma, and is characterized by excellent hepatic arterial enhancement with good portal vein enhancement, but no forward enhancement of the hepatic veins(23, 24) (Figure 2). In comparison, the early arterial phase shows enhancement of the hepatic arteries without significant contrast in the portal or hepatic veins and generally does not show hypervascular lesions well(23). Because the late arterial phase is well-established for the detection of arterial phase hyperenhancing lesions, we use the term “arterial phase” to specifically refer to the late arterial phase in our article.

Unlike MRI and US, which allow multiple arterial phase images to be acquired without a radiation dose penalty, CT imaging requires accurate scan delay timing to capture a single optimal arterial phase consistently. Unlike the other phases of enhancement (noncontrast, portal venous, and delayed phases), the late arterial phase occurs in a brief moment -- mis-timing can render a liver CT scan insufficient for HCC or other hyperenhancing lesion detection and staging. For this reason, we recommend that late arterial phase scan protocols should be patient-specific (Tables 2a-2c) and use rapid bolus injections of large contrast material doses followed by a rapid bolus injection of saline to flush contrast agent into the general circulation(25). Fixed scan delays do not account for inter-individual comorbidities or catheter placement issues which often profoundly affect contrast arrival time in the liver. We recommend the test-bolus method which aims for an optimal scan but is more time-consumimg or the bolus-tracking method which aims for a good scan and is more automated. Both of these patient-specific methods monitor the abdominal aorta every 1 to 2 seconds with low mA technique and have proven robust in clinical practice.

Given the relative importance of the late arterial phase, some practices utilize higher radiation dose to achieve lower image noise for this critical phase than for other phases of a liver CT exam.

Portal Venous Phase

The portal venous phase of CT liver imaging typically occurs at 60 to 90 seconds after the start of IV contrast injection and is characterized by full enhancement of the portal veins and hepatic arteries, forward enhancement of the hepatic veins, and bright liver parenchymal enhancement. This phase of contrast optimally displays hypovascular metastases and biliary abnormalities (26, 27) and may be better than the arterial phase in detecting residual disease enhancement after arterial embolization for the treatment of HCC (28). Washout in HCC may be seen on this phase, but is often better seen on the delayed phase (Figure 3). Timing of the portal venous phase is more forgiving than for the arterial phase, but erring on slightly late acquisition (80 seconds) may be better than acquisition that is too early. When using a timing bolus for the arterial phase, the optimal portal venous phase scan delay may also be calculated(29, 30) (Table 2c).

Delayed Phase

The delayed phase, also known as the “equilibrium phase” is obtained at 3 to 5 minutes after contrast injection. During this phase, contrast has equilibrated between the intravascular and interstitial water of the liver, such as in areas of liver fibrosis. The delayed phase is the optimal phase for the detection of washout, capsule appearance, and mosaic architecture of HCC, particularly in small < 2 cm lesions (Figure 3) (26, 27, 31–33). Multiple studies have shown that the use of delayed phase increases the detection of and confidence in the diagnosis of HCC, and increases the rate of detection of hypovascular tumors and cholangiocarcinomas (26, 27, 31–33).

Dual Energy CT

DECT is a valuable tool for liver imaging that can brighten contrast attenuation, reduce artifacts, and increase lesion detection. DECT exploits the fact that all materials attenuate X-rays to a degree unique to that material at low versus high energy. Unlike conventional CT [single energy CT (SECT)], DECT obtains two separate sets of CT data, one from low and one from high energy X-ray photon spectra(34). In particular, iodine contrast can be delineated from calcium and organic material by DECT, even if they have similar HU values at SECT.

Image Reconstructions

Various vendor-specific implementations of DECT are available, and a detailed discussion on each of these is beyond the scope of this review article. Nevertheless, all clinical DECT systems produce similar image reconstructions. The DECT image reconstructions most relevant to liver imaging are 120-kVp-like images which closely resemble conventional SECT scans, virtual unenhanced images (VUE), virtual monochromatic images (VMC), and material-specific images, particularly the iodine image(34, 35).

VUE Images

VUE images resemble true noncontrast scans in appearance (36, 37). VUE images can help differentiate calcium and hemorrhage from iodine enhancement in a lesion or liver tissue to aid diagnosis and allow elimination of a separate noncontrast CT, which simplifies multiphase CT and reduces radiation dose exposure(35). Although early results are encouraging, the attenuation values on VUE images may depend on the dual-energy scanner, patient's body habitus, and the acquisition phase of the DECT protocol(38). Incomplete iodine subtraction and inability to measure HU value on some vendor-specific VUE images are other challenges(35, 38). Also, lipiodol chemoembolization material in a treated lesion may be subtracted on VUE and hence may be mistaken for contrast enhancement(39). For the evaluation of ambiguous high attenuation foci, VNC images should always be viewed alongside iodine and 120-kVp-like images.

VMC Images

VMC images simulate the appearance of a CT scan acquired with a monochromatic X-ray beam at a given X-ray energy (keV)(40). These images resemble 120-kVp single energy CT (SECT) images but with increased attenuation of iodine contrast when reconstructed at low keV (<60 keV), and reduced beam hardening artifact at high keV (>80 keV)(40). Low keV VMC images (<55 keV) can improve the conspicuity of hypervascular liver lesions (Figure 4) (41) and may be helpful to "rescue" CT scans with poor contrast enhancement such as from a poor bolus(42). Portal venous phase DECT scans may benefit from low keV VMC images to better delineate hypovascular lesions such as metastases and infiltrating liver masses(41, 43).

Iodine images

Iodine images show the distribution of iodine contrast and can be displayed as a gray-scale image or as a color-coded overlay on the 120-kVp-like image(44). In comparison to the iodine enhancement assessment on SECT, iodine images and low keV images provide better image contrast and more reliable measurement of tissue enhancement(45) (Figure 5 and 6). When viewed in conjunction with VNC images, tissue enhancement can be determined without the need for true noncontrast images (Figure 6). For example, calcified lesions may be differentiated from enhancing masses and tumor thrombi may be differentiated from bland thrombi. (46). Early reports suggest that the use of DECT iodine concentration may be better than SECT as an imaging biomarker of HCC response to local therapy (47) (48) Figure 6.

Diffuse liver disease

Diffuse liver disease is an important public health problem and a major cause of liver-related morbidity and mortality in the United States and worldwide (49). Steatosis, iron deposition, inflammation, and cholestasis can lead to diffuse liver parenchymal injury, which if untreated, may progress to cirrhosis and its complications (50). Liver biopsy remains the reference standard for diffuse liver disease diagnosis, but is invasive, can be limited by sampling error, and not feasible for monitoring treatment and long-term clinical follow-up(51). Non-invasive imaging by MRI is the most accurate for liver fat and fibrosis

quantification, and US is valuable for fat and fibrosis quantification. Nevertheless, CT is commonly obtained, highly reproducible, and may be obtained in circumstances when patients are unable to undergo MRI.

Liver Steatosis and Iron Deposition

Liver steatosis is associated with metabolic X syndrome and non-alcoholic fatty liver disease (NAFLD) which may progress to steatohepatitis and cirrhosis(52). Liver iron overload may be primary (idiopathic) or secondary and, if untreated, can lead to cirrhosis and multiorgan failure(53). A concern for CT assessment of fat and iron deposition is these two materials have opposite effects on CT attenuation such that the presence of one may interfere with the assessment of the other: fat decreases and iron increases liver attenuation. While SECT may not be sensitive for the detection of mild steatosis, several noncontrast 120-kVp SECT thresholds (e.g. <37 or <48 HU) have shown value for the detection of moderate to severe steatosis (≥30% fat at histology)(54). Conversely, the noncontrast SECT thresholds for iron overload (e.g. >75 HU) are suggestive but nonspecific since high liver CT attenuation may be seen in other scenarios such as treatment with amiodarone or colloidal gold, Wilson's disease, and glycogen storage disease. When intravenous contrast is given for SECT, the detection of steatosis or iron deposition becomes even less accurate.

To an extent, DECT mitigates some of the limitations of SECT since material decomposition may allow for more specific quantification of either fat or iron. Unlike water and normal liver tissue which show negligible changes in the attenuation at different kVp settings, the liver attenuation varies linearly with varying degrees of liver iron overload and steatosis. In cases of steatosis, the CT attenuation increases with higher kVp imaging. Conversely, in cases of iron deposition, the CT attenuation decreases slightly with higher kVp imaging. But clinical study results for DECT quantification of deposition disease have been mixed particularly for low level steatosis and iron deposition (55–58)(Table 5). Better results are seen with DECT quantification of liver iron in patients with moderate to severe iron overload, which is a population where MRI quantification is less accurate(59–62). Potentially, newer multi-material decomposition algorithms may allow for differentiation of iron from other materials including fat, and large-cohort clinical studies for the validation of DECT is warranted.

Liver Fibrosis

Liver fibrosis results from repeated injury to the liver. Fibrosis staging carries important prognostic implications as early stage can be treated and even reversed with anti-viral therapy for hepatitis B or C infections and lifestyle modifications in nonalcoholic steatohepatitis (NASH) (63). Among imaging techniques, MRI, and ultrasound elastography are most commonly used in clinical practice(64). Nevertheless, several CT methods of staging fibrosis are being studied. Morphologic measures of fibrosis include liver segmental volume ratio(65) and liver surface nodularity score which are simple methods but may require specialized software(66). Contrast-enhanced CT methods include perfusion CT which can show correlation of contrast mean transient time and arterial fractional flow with fibrosis stage. Such methods require dedicated CT protocols, high radiation dose, and software. Simpler measurement of the hepatic extracellular volume fraction (fECV)

on equilibrium and noncontrast phases, as calculated by the formula - fECV (%) = liver enhancement/aorta enhancement × (100 - Hematocrit [%]), showed good prediction of cirrhosis and modest prediction of fibrosis stage at routine imaging(64, 67). DECT further simplifies fECV calculation from a single equilibrium (delayed) phase scan without need for an additional unenhanced scan(68). Further studies are needed to validate the role of DECT to quantify liver fibrosis.

Future directions

Several advances in CT loom on the horizon and promise to be available within the next 5 to 10 years. Artificial intelligence (AI) is already changing radiology practice(69) and will improve many basic aspects of our specialty. Deep learning using convolutional neural networks (CNNs) is used to reduce image noise, reduce required radiation dose, increase contrast attenuation, and reduce artifacts at CT(3, 70). (Figure 7). Deep learning in image recognition promises to reduce radiologist workload and improve diagnostic consistency(69) for detecting and characteriaing focal(71) (72) and diffuse liver diseases(73).

Photon-counting Computed Tomography (PCCT) utilizes tiny detectors that sort incident photons by energy. Theoretically, these small detectors should provide superior spatial resolution, reduce required radiation dose, reduce beam hardening artifact, and provide more detailed spectral delineation of the imaged body parts than possible with existing clinical CT scanners which all use energy-integrating detectors(74, 75). PCCT, should enable the reconstruction of more accurate material-specific maps and differentiate more than two materials(74), such as needed for the quantification of hepatic steatosis, iron, and contrast enhancement. In parallel, novel non-iodine contrast agents are under development that can be given simultaneously with iodine agents yet appear as different “colors” at DECT and even more vivdly at PCCT(74, 76) These contrast agents generally utilize high atomic number reporter atoms, such as tantalum, bismuth, gold, ytterbium, or hafnium and may provide CT attenuation benefits even with SECT(77). Multi-contrast PCCT exams, such as with iodine and gadolinium contrast agents in a single acquisition could provide both the arterial and venous phase exam of the liver with perfect image co-registration(76, 78). Of course, such images would further improve the value of AI for liver CT analysis.

Conclusion

CT remains a cornerstone of liver disease evaluation. Wide-detector and dual-energy CT technologies allow for improved detection and characterization of focal liver lesions and, to a lesser extent, assessment of liver steatosis, iron deposition, and fibrosis. Attention to CT technique, and in particular accurately capturing the late arterial phase, improves the evaluation for HCC and other hypervascular tumors. Emerging technologies including artificial intelligence, photon counting CT, and novel contrast agents will further improve the capabilities of liver CT diagnoses.

Acknowledgments

Disclosures:

NK: Consultant for GE Healthcare

AK: Research Grant – GE Healthcare, Philips Healthcare, PanCAN

AF: No disclosures

BMY: Grants from General Electric Healthcare, Philips Healthcare, Guerbet, NIH; Shareholder of Nextrast; Consultant for General Electric Healthcare; Speaker for General Electric Healthcare, Philips Healthcare, Canon Medical Systems; Book royalties from Oxford University Press. Patent royalties from UCSF.

Abbreviations

AI	artificial intelligence
ATCM	automatic tube current modulation
cm	centimeters
CNNs	convolutional neural networks
CT	computed tomography
DECT	dual energy CT
DLIR	Deep learning image reconstruction
dl-DECT	dual layer detector DECT
ds-DECT	dual source DECT
IV	intravenous
HCC	hepatocellular carcinoma
HU	Hounsfield Unit
keV	kiloelectron volt
kVp	kilovoltage peak
LI-RADS	Liver Reporting & Data System
mA	milliampere
mm	millimeters
MRI	Magnetic Resonance Imaging
NAFLD	non-alcoholic fatty liver disease
PCCT	photon counting
CT sec	seconds
SECT	single energy CT (conventional CT)
ss-DECT	single source DECT

US	ultrasound
VIC	Virtual iron content
VMC	virtual monochromatic
VUE	virtual unenhanced

References

1. Boll DT, Merkle EM. Diffuse liver disease: strategies for hepatic CT and MR imaging. Radiographics. 2009;29(6):1591–614. [PubMed: 19959510]
2. McCollough CH, Leng S, Yu L, Fletcher JG. Dual- and Multi-Energy CT: Principles, Technical Approaches, and Clinical Applications. Radiology. 2015;276(3):637–53. [PubMed: 26302388]
3. Lell MM, Kachelriess M. Recent and Upcoming Technological Developments in Computed Tomography: High Speed, Low Dose, Deep Learning, Multienergy. Invest Radiol. 2020;55(1):8–19. [PubMed: 31567618]
4. Ginat DT, Gupta R. Advances in computed tomography imaging technology. Annu Rev Biomed Eng. 2014;16:431–53. [PubMed: 25014788]
5. Juan C. Ramirez-Giraldo MF, Katharine Grant, Andrew N. Primak, Thomas FlohrNew Approaches to Reduce Radiation While Maintaining Image Quality in Multi-Detector-Computed Tomography. Current Radiology Reports. 2015;3.
6. Soloff EV, Desai N, Busey JM, Koprowicz KM, Shuman WP. Feasibility of wide detector three-pass arterial phase liver CT in patients with cirrhosis: timing of hyperenhancing lesion peak conspicuity. Abdom Radiol (NY). 2020;45(8):2370–7. [PubMed: 32333072]
7. Fang W, Wang CH, Yu YF, et al.The feasibility of 1-stop examination of coronary CT angiography and abdominal enhanced CT. Medicine (Baltimore). 2018;97(32):e11651.
8. Palorini F, Origgi D, Granata C, Matranga D, Salerno S. Adult exposures from MDCT including multiphase studies: first Italian nationwide survey. Eur Radiol. 2014;24(2):469–83. [PubMed: 24121713]
9. Israel GM, Cicchiello L, Brink J, Huda W. Patient size and radiation exposure in thoracic, pelvic, and abdominal CT examinations performed with automatic exposure control. AJR Am J Roentgenol. 2010;195(6):1342–6. [PubMed: 21098193]
10. Kalra MK, Maher MM, Toth TL, Kamath RS, Halpern EF, Saini S. Comparison of Z-axis automatic tube current modulation technique with fixed tube current CT scanning of abdomen and pelvis. Radiology. 2004;232(2):347–53. [PubMed: 15286306]
11. Yeh BM, Shepherd JA, Wang ZJ, Teh HS, Hartman RP, Prevrhal S. Dual-energy and low-kVp CT in the abdomen. AJR Am J Roentgenol. 2009;193(1):47–54. [PubMed: 19542394]
12. Lee KH, Lee JM, Moon SK, et al.Attenuation-based automatic tube voltage selection and tube current modulation for dose reduction at contrast-enhanced liver CT. Radiology. 2012;265(2):437–47. [PubMed: 23012467]
13. Marin D, Nelson RC, Schindera ST, et al.Low-tube-voltage, high-tube-current multidetector abdominal CT: improved image quality and decreased radiation dose with adaptive statistical iterative reconstruction algorithm--initial clinical experience. Radiology. 2010;254(1):145–53. [PubMed: 20032149]
14. Desai GS, Uppot RN, Yu EW, Kambadakone AR, Sahani DV. Impact of iterative reconstruction on image quality and radiation dose in multidetector CT of large body size adults. Eur Radiol. 2012;22(8):1631–40. [PubMed: 22527370]
15. Seyal AR, Arslanoglu A, Abboud SF, Sahin A, Horowitz JM, Yaghmai V. CT of the Abdomen with Reduced Tube Voltage in Adults: A Practical Approach. Radiographics. 2015;35(7):1922–39. [PubMed: 26473536]
16. Prakash P, Kalra MK, Kambadakone AK, et al.Reducing abdominal CT radiation dose with adaptive statistical iterative reconstruction technique. Invest Radiol. 2010;45(4):202–10. [PubMed: 20177389]

17. Mileto A, Guimaraes LS, McCollough CH, Fletcher JG, Yu L. State of the Art in Abdominal CT: The Limits of Iterative Reconstruction Algorithms. Radiology. 2019;293(3):491–503. [PubMed: 31660806]
18. Chung BM, Park HJ, Park SB, Lee JB, Ahn HS, Kim YS. Differentiation of small arterial enhancing hepatocellular carcinoma from non-tumorous arterioportal shunt with an emphasis on the precontrast CT scan. Abdom Imaging. 2015;40(7):2200–9. [PubMed: 25916870]
19. Hennedige T, Yang ZJ, Ong CK, Venkatesh SK. Utility of non-contrast-enhanced CT for improved detection of arterial phase hyperenhancement in hepatocellular carcinoma. Abdom Imaging. 2014;39(6):1247–54. [PubMed: 24943135]
20. Kim HC, Kim AY, Han JK, et al.Hepatic arterial and portal venous phase helical CT in patients treated with transcatheter arterial chemoembolization for hepatocellular carcinoma: added value of unenhanced images. Radiology. 2002;225(3):773–80. [PubMed: 12461260]
21. Brink JA. Use of high concentration contrast media (HCCM): principles and rationale--body CT. Eur J Radiol. 2003;45 Suppl 1:S53–8. [PubMed: 12598028]
22. Heiken JP, Brink JA, McClennan BL, Sagel SS, Crowe TM, Gaines MV. Dynamic incremental CT: effect of volume and concentration of contrast material and patient weight on hepatic enhancement. Radiology. 1995;195(2):353–7. [PubMed: 7724752]
23. Laghi A, Iannaccone R, Rossi P, et al.Hepatocellular carcinoma: detection with triple-phase multi-detector row helical CT in patients with chronic hepatitis. Radiology. 2003;226(2):543–9. [PubMed: 12563152]
24. Ichikawa T, Kitamura T, Nakajima H, et al.Hypervascular hepatocellular carcinoma: can double arterial phase imaging with multidetector CT improve tumor depiction in the cirrhotic liver?AJR Am J Roentgenol. 2002;179(3):751–8. [PubMed: 12185057]
25. Bae KT. Intravenous contrast medium administration and scan timing at CT: considerations and approaches. Radiology. 2010;256(1):32–61. [PubMed: 20574084]
26. Liu YI, Kamaya A, Jeffrey RB, Shin LK. Multidetector computed tomography triphasic evaluation of the liver before transplantation: importance of equilibrium phase washout and morphology for characterizing hypervascular lesions. J Comput Assist Tomogr. 2012;36(2):213–9. [PubMed: 22446362]
27. Lim JH, Choi D, Kim SH, et al.Detection of hepatocellular carcinoma: value of adding delayed phase imaging to dual-phase helical CT. AJR Am J Roentgenol. 2002;179(1):67–73. [PubMed: 12076907]
28. Lam A, Fernando D, Sirlin CC, et al.Value of the portal venous phase in evaluation of treated hepatocellular carcinoma following transcatheter arterial chemoembolisation. Clin Radiol. 2017;72(11):994 e9- e16.
29. Chu LL, Joe BN, Westphalen AC, Webb EM, Coakley FV, Yeh BM. Patient-specific time to peak abdominal organ enhancement varies with time to peak aortic enhancement at MR imaging. Radiology. 2007;245(3):779–87. [PubMed: 17911535]
30. Schneider JG, Wang ZJ, Wang W, Yee J, Fu Y, Yeh BM. Patient-tailored scan delay for multiphase liver CT: improved scan quality and lesion conspicuity with a novel timing bolus method. AJR Am J Roentgenol. 2014;202(2):318–23. [PubMed: 24450671]
31. Iannaccone R, Laghi A, Catalano C, et al.Hepatocellular carcinoma: role of unenhanced and delayed phase multi-detector row helical CT in patients with cirrhosis. Radiology. 2005;234(2):460–7. [PubMed: 15671002]
32. Liu YI, Shin LK, Jeffrey RB, Kamaya A. Quantitatively defining washout in hepatocellular carcinoma. AJR Am J Roentgenol. 2013;200(1):84–9. [PubMed: 23255745]
33. Monzawa S, Ichikawa T, Nakajima H, Kitanaka Y, Omata K, Araki T. Dynamic CT for detecting small hepatocellular carcinoma: usefulness of delayed phase imaging. AJR Am J Roentgenol. 2007;188(1):147–53. [PubMed: 17179357]
34. De Cecco CN, Darnell A, Rengo M, et al.Dual-energy CT: oncologic applications. AJR Am J Roentgenol. 2012;199(5 Suppl):S98–S105. [PubMed: 23097174]
35. Morgan DE. Dual-energy CT of the abdomen. Abdom Imaging. 2014;39(1):108–34. [PubMed: 24072382]

36. Zhang LJ, Peng J, Wu SY, et al.Liver virtual non-enhanced CT with dual-source, dual-energy CT: a preliminary study. Eur Radiol. 2010;20(9):2257–64. [PubMed: 20393717]
37. De Cecco CN, Muscogiuri G, Schoepf UJ, et al.Virtual unenhanced imaging of the liver with third-generation dual-source dual-energy CT and advanced modeled iterative reconstruction. Eur J Radiol. 2016;85(7):1257–64. [PubMed: 27235872]
38. De Cecco CN, Darnell A, Macias N, et al.Virtual unenhanced images of the abdomen with second-generation dual-source dual-energy computed tomography: image quality and liver lesion detection. Invest Radiol. 2013;48(1):1–9. [PubMed: 23070097]
39. Lee JM, Yoon JH, Joo I, Woo HS. Recent Advances in CT and MR Imaging for Evaluation of Hepatocellular Carcinoma. Liver Cancer. 2012;1(1):22–40. [PubMed: 24159569]
40. Yu L, Leng S, McCollough CH. Dual-energy CT-based monochromatic imaging. AJR Am J Roentgenol. 2012;199(5 Suppl):S9–S15. [PubMed: 23097173]
41. Yamada Y, Jinzaki M, Tanami Y, Abe T, Kuribayashi S. Virtual monochromatic spectral imaging for the evaluation of hypovascular hepatic metastases: the optimal monochromatic level with fast kilovoltage switching dual-energy computed tomography. Invest Radiol. 2012;47(5):292–8. [PubMed: 22472797]
42. Lv P, Zhou Z, Liu J, et al.Can virtual monochromatic images from dual-energy CT replace low-kVp images for abdominal contrast-enhanced CT in small- and medium-sized patients?Eur Radiol. 2019;29(6):2878–89. [PubMed: 30506223]
43. Caruso D, De Cecco CN, Schoepf UJ, et al.Can dual-energy computed tomography improve visualization of hypoenhancing liver lesions in portal venous phase? Assessment of advanced image-based virtual monoenergetic images. Clin Imaging. 2017;41:118–24. [PubMed: 27840263]
44. Patino M, Prochowski A, Agrawal MD, et al.Material Separation Using Dual-Energy CT: Current and Emerging Applications. Radiographics. 2016;36(4):1087–105. [PubMed: 27399237]
45. Agrawal MD, Pinho DF, Kulkarni NM, Hahn PF, Guimaraes AR, Sahani DV. Oncologic applications of dual-energy CT in the abdomen. Radiographics. 2014;34(3):589–612. [PubMed: 24819783]
46. Qian LJ, Zhu J, Zhuang ZG, et al.Differentiation of neoplastic from bland macroscopic portal vein thrombi using dual-energy spectral CT imaging: a pilot study. Eur Radiol. 2012;22(10):2178–85. [PubMed: 22622347]
47. Lee JA, Jeong WK, Kim Y, et al.Dual-energy CT to detect recurrent HCC after TACE: initial experience of color-coded iodine CT imaging. Eur J Radiol. 2013;82(4):569–76. [PubMed: 23238365]
48. Lee SH, Lee JM, Kim KW, et al.Dual-energy computed tomography to assess tumor response to hepatic radiofrequency ablation: potential diagnostic value of virtual noncontrast images and iodine maps. Invest Radiol. 2011;46(2):77–84. [PubMed: 20856125]
49. Schuppan D, Afdhal NH. Liver cirrhosis. Lancet. 2008;371(9615):838–51. [PubMed: 18328931]
50. Chalasani N, Younossi Z, Lavine JE, et al.The diagnosis and management of nonalcoholic fatty liver disease: Practice guidance from the American Association for the Study of Liver Diseases. Hepatology. 2018;67(1):328–57. [PubMed: 28714183]
51. Kose S, Ersan G, Tatar B, Adar P, Sengel BE. Evaluation of Percutaneous Liver Biopsy Complications in Patients with Chronic Viral Hepatitis. Eurasian J Med. 2015;47(3):161–4. [PubMed: 26644763]
52. Fotbolcu H, Zorlu E. Nonalcoholic fatty liver disease as a multi-systemic disease. World J Gastroenterol. 2016;22(16):4079–90. [PubMed: 27122660]
53. Adams P, Brissot P, Powell LW. EASL International Consensus Conference on Haemochromatosis. J Hepatol. 2000;33(3):485–504. [PubMed: 11020008]
54. Pickhardt PJ, Park SH, Hahn L, Lee SG, Bae KT, Yu ES. Specificity of unenhanced CT for noninvasive diagnosis of hepatic steatosis: implications for the investigation of the natural history of incidental steatosis. Eur Radiol. 2012;22(5):1075–82. [PubMed: 22138733]
55. Zheng X, Ren Y, Phillips WT, et al.Assessment of hepatic fatty infiltration using spectral computed tomography imaging: a pilot study. J Comput Assist Tomogr. 2013;37(2):134–41. [PubMed: 23493199]

56. Hyodo T, Hori M, Lamb P, et al.Multimaterial Decomposition Algorithm for the Quantification of Liver Fat Content by Using Fast-Kilovolt-Peak Switching Dual-Energy CT: Experimental Validation. Radiology. 2017;282(2):381–9. [PubMed: 27541687]
57. Patel BN, Kumbla RA, Berland LL, Fineberg NS, Morgan DE. Material density hepatic steatosis quantification on intravenous contrast-enhanced rapid kilovolt (peak)-switching single-source dual-energy computed tomography. J Comput Assist Tomogr. 2013;37(6):904–10. [PubMed: 24270112]
58. Kramer H, Pickhardt PJ, Kliewer MA, et al.Accuracy of Liver Fat Quantification With Advanced CT, MRI, and Ultrasound Techniques: Prospective Comparison With MR Spectroscopy. AJR Am J Roentgenol. 2017;208(1):92–100. [PubMed: 27726414]
59. Joe E, Kim SH, Lee KB, et al.Feasibility and accuracy of dual-source dual-energy CT for noninvasive determination of hepatic iron accumulation. Radiology. 2012;262(1):126–35. [PubMed: 22106352]
60. Luo XF, Xie XQ, Cheng S, et al.Dual-Energy CT for Patients Suspected of Having Liver Iron Overload: Can Virtual Iron Content Imaging Accurately Quantify Liver Iron Content?Radiology. 2015;277(1):95–103. [PubMed: 25880263]
61. Ma J, Song ZQ, Yan FH. Separation of hepatic iron and fat by dual-source dual-energy computed tomography based on material decomposition: an animal study. PLoS One. 2014;9(10):e110964.
62. Werner S, Krauss B, Haberland U, et al.Dual-energy CT for liver iron quantification in patients with haematological disorders. Eur Radiol. 2019;29(6):2868–77. [PubMed: 30406312]
63. Lee YA, Wallace MC, Friedman SL. Pathobiology of liver fibrosis: a translational success story. Gut. 2015;64(5):830–41. [PubMed: 25681399]
64. Horowitz JM, Venkatesh SK, Ehman RL, et al.Evaluation of hepatic fibrosis: a review from the society of abdominal radiology disease focus panel. Abdom Radiol (NY). 2017;42(8):2037–53. [PubMed: 28624924]
65. Furusato Hunt OM, Lubner MG, Ziemlewicz TJ, Munoz Del Rio A, Pickhardt PJ. The Liver Segmental Volume Ratio for Noninvasive Detection of Cirrhosis: Comparison With Established Linear and Volumetric Measures. J Comput Assist Tomogr. 2016;40(3):478–84. [PubMed: 26966951]
66. Smith AD, Branch CR, Zand K, et al.Liver Surface Nodularity Quantification from Routine CT Images as a Biomarker for Detection and Evaluation of Cirrhosis. Radiology. 2016;280(3):771–81. [PubMed: 27089026]
67. Varenika V, Fu Y, Maher JJ, et al.Hepatic fibrosis: evaluation with semiquantitative contrast-enhanced CT. Radiology. 2013;266(1):151–8. [PubMed: 23169796]
68. Lamb P, Sahani DV, Fuentes-Orrego JM, Patino M, Ghosh A, Mendonca PR. Stratification of patients with liver fibrosis using dual-energy CT. IEEE Trans Med Imaging. 2015;34(3):807–15. [PubMed: 25181365]
69. Hosny A, Parmar C, Quackenbush J, Schwartz LH, Aerts H. Artificial intelligence in radiology. Nat Rev Cancer. 2018;18(8):500–10. [PubMed: 29777175]
70. Higaki T, Nakamura Y, Tatsugami F, Nakaura T, Awai K. Improvement of image quality at CT and MRI using deep learning. Jpn J Radiol. 2019;37(1):73–80. [PubMed: 30498876]
71. Vivanti R, Szeskin A, Lev-Cohain N, Sosna J, Joskowicz L. Automatic detection of new tumors and tumor burden evaluation in longitudinal liver CT scan studies. Int J Comput Assist Radiol Surg. 2017;12(11):1945–57. [PubMed: 28856515]
72. Yasaka K, Akai H, Abe O, Kiryu S. Deep Learning with Convolutional Neural Network for Differentiation of Liver Masses at Dynamic Contrast-enhanced CT: A Preliminary Study. Radiology. 2018;286(3):887–96. [PubMed: 29059036]
73. Choi KJ, Jang JK, Lee SS, et al.Development and Validation of a Deep Learning System for Staging Liver Fibrosis by Using Contrast Agent-enhanced CT Images in the Liver. Radiology. 2018;289(3):688–97. [PubMed: 30179104]
74. Willemink MJ, Persson M, Pourmorteza A, Pelc NJ, Fleischmann D. Photon-counting CT: Technical Principles and Clinical Prospects. Radiology. 2018;289(2):293–312. [PubMed: 30179101]

75. Symons R, Reich DS, Bagheri M, et al.Photon-Counting Computed Tomography for Vascular Imaging of the Head and Neck: First In Vivo Human Results. Invest Radiol. 2018;53(3):135–42. [PubMed: 28926370]

76. Symons R, Krauss B, Sahbaee P, et al.Photon-counting CT for simultaneous imaging of multiple contrast agents in the abdomen: An in vivo study. Med Phys. 2017;44(10):5120–7. [PubMed: 28444761]

77. Yeh BM, FitzGerald PF, Edic PM, et al.Opportunities for new CT contrast agents to maximize the diagnostic potential of emerging spectral CT technologies. Adv Drug Deliv Rev. 2017;113:201–22. [PubMed: 27620496]

78. Si-Mohamed S, Thivolet A, Bonnot PE, et al.Improved Peritoneal Cavity and Abdominal Organ Imaging Using a Biphasic Contrast Agent Protocol and Spectral Photon Counting Computed Tomography K-Edge Imaging. Invest Radiol. 2018;53(10):629–39. [PubMed: 29794948]

key points:

- Attention to technique for the late arterial phase is critical for evaluation of possible arterial phase hyperenhancing lesions
- Delayed phase imaging provides superior assessment of washout compared to portal venous phase imaging
- CT technology is advancing rapidly.

Key Point:

Achieving an optimal late arterial phase scan is critical for the detection of hypervascular liver lesions

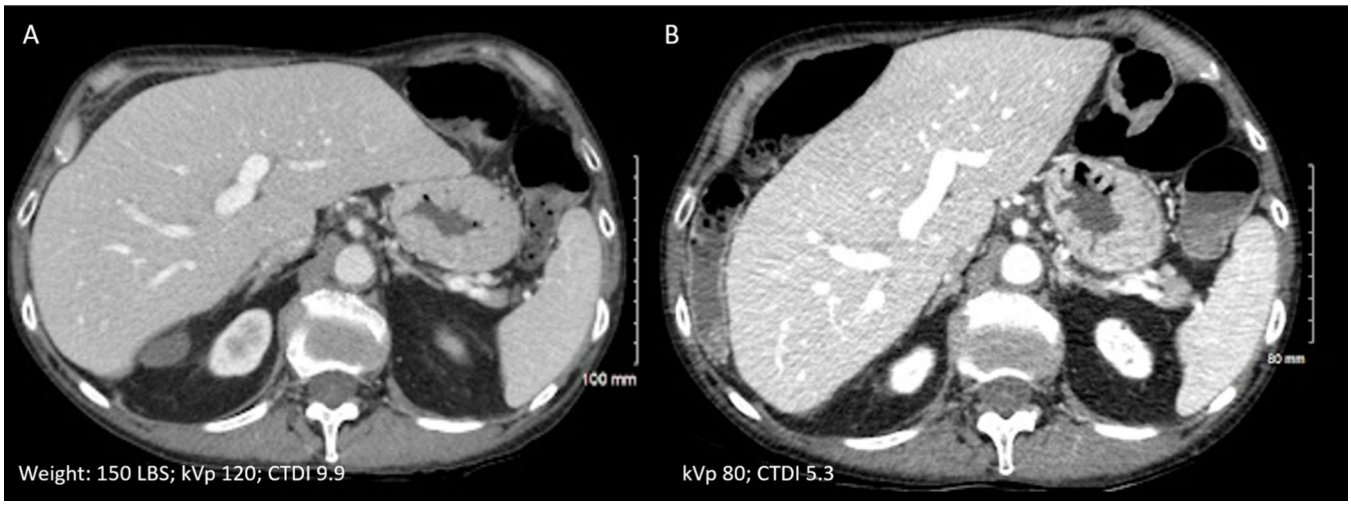

Figure 1: Low kVp technique.

Contrast enhanced portal venous phase images of a patient acquired at a) 120kVp and b) 80 kVp setting (three months apart). By use of 80kVp and iterative reconstruction technique (ASiR-V), almost 50% radiation dose reduction was achieved with minimal increase in image noise and with improved contrast attenuation.

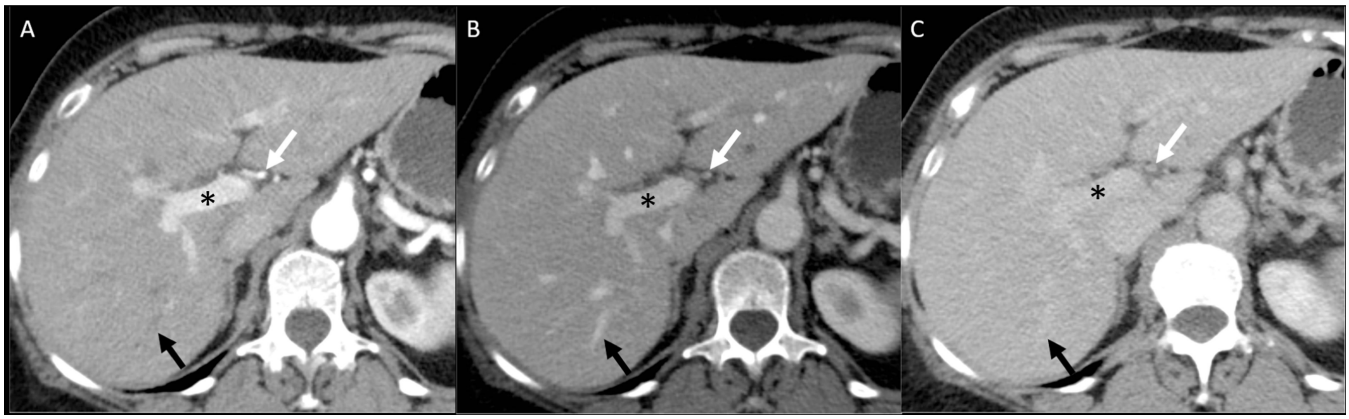

Figure 2: Multiphase liver CT protocol for HCC.

Late arterial (A), portal venous (B), and equilibrium (C) phases. The hepatic late arterial phase is when the hepatic artery (white arrows) is fully enhanced with good portal vein (*) enhancement, but without visible antegrade hepatic vein enhancement (black arrows). During the portal venous phase, the hepatic arteries, portal veins, and hepatic veins are all well-enhanced. During the equilibrium phase, also known as the delayed phase, the contrast enhancement of all vessels is uniform and contrast has largely equilibrated with the interstitial space of the liver parenchyma.

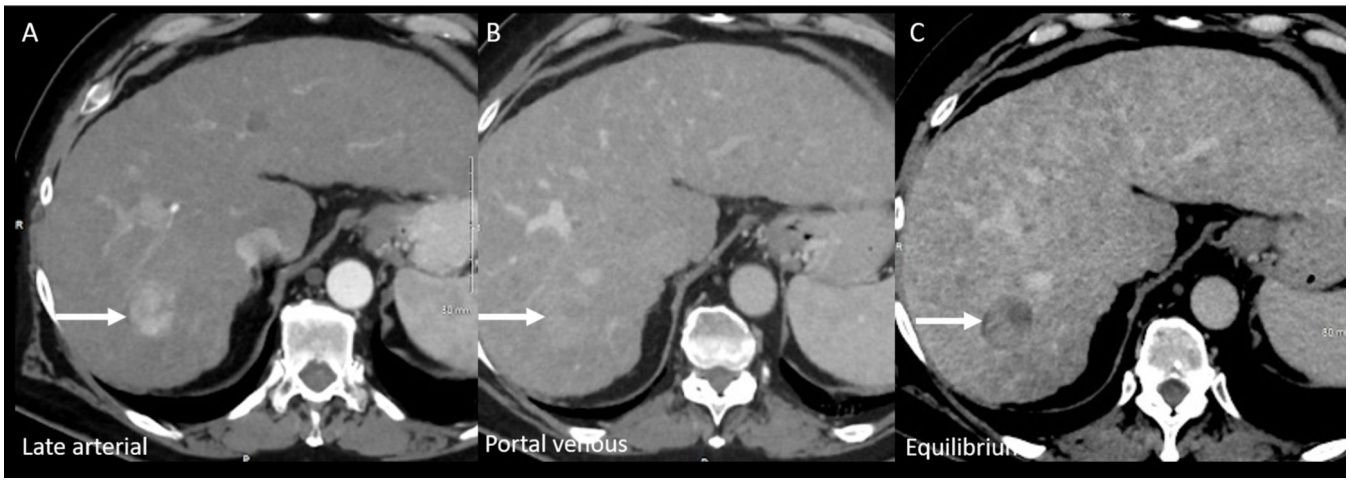

Figure 3: HCC on multiphase CT.

HCC (arrow) on the late arterial (A), portal venous (B) and equilibrium phases. Although faint washout is seen on portal venous phase, the tumor washout and pseudocapsule features are best seen on the equilibrium phase. This case shows the importance of including an equilibrium phase for the evaluation of HCC.

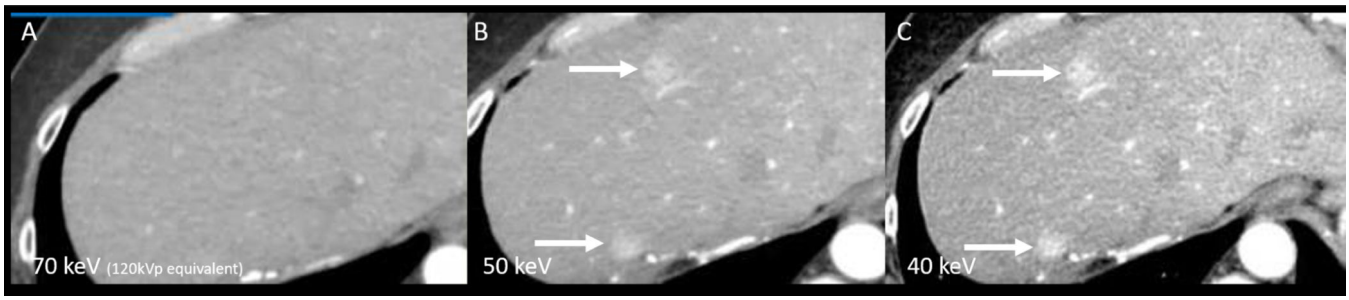

Figure 4: DECT Low energy VMC images improve lesion conspicuity.

Axial contrast enhanced DECT VMC images at the level of liver obtained during late arterial phase of contrast enhancement. Two hypervascular liver metastases (arrows) are barely seen on the 70keV VMC image (A) and are more conspicuous on the 50keV (B) and 40keV (C) VMC images.

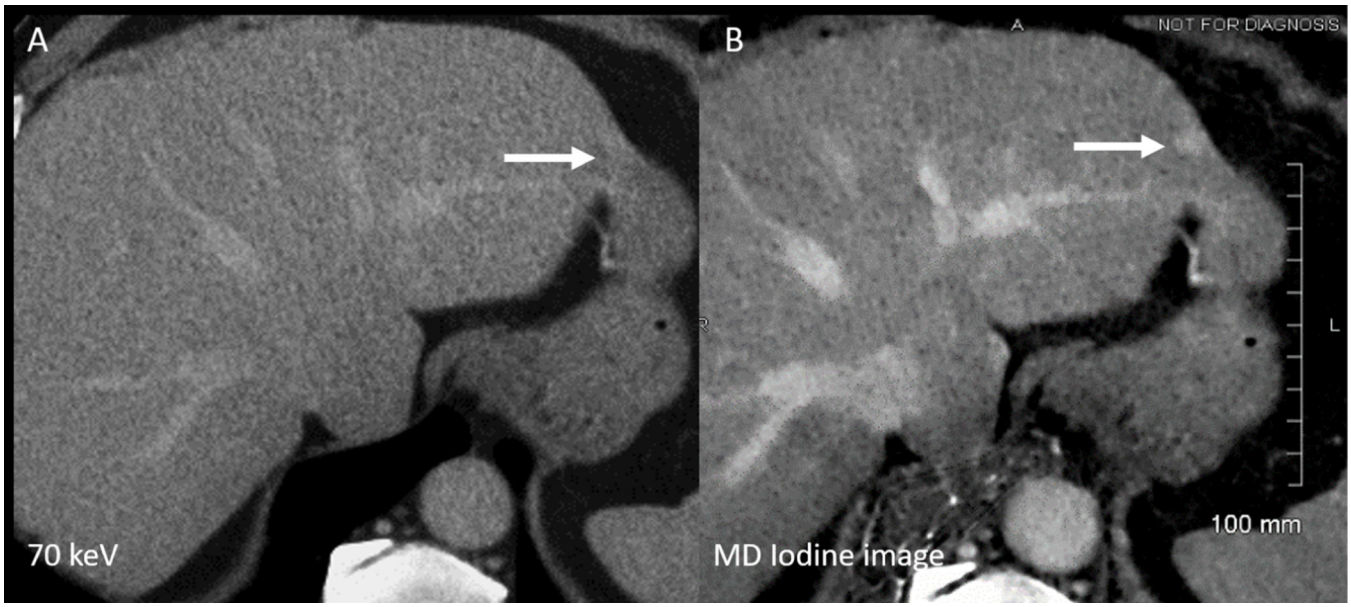

Figure 5: Improved lesion visibility on material density (MD) iodine image.

Axial contrast enhanced 70 keV (A) and iodine (B) images of the liver obtained during portal venous of contrast enhancement. An incidental small lesion in the left lobe lateral segment is better seen on iodine image due to its inherent superior contrast. Although the lesion eventually turned out to be a hemangioma (on MR not shown here), this example highlights the benefit of iodine images for the detection of small lesions.

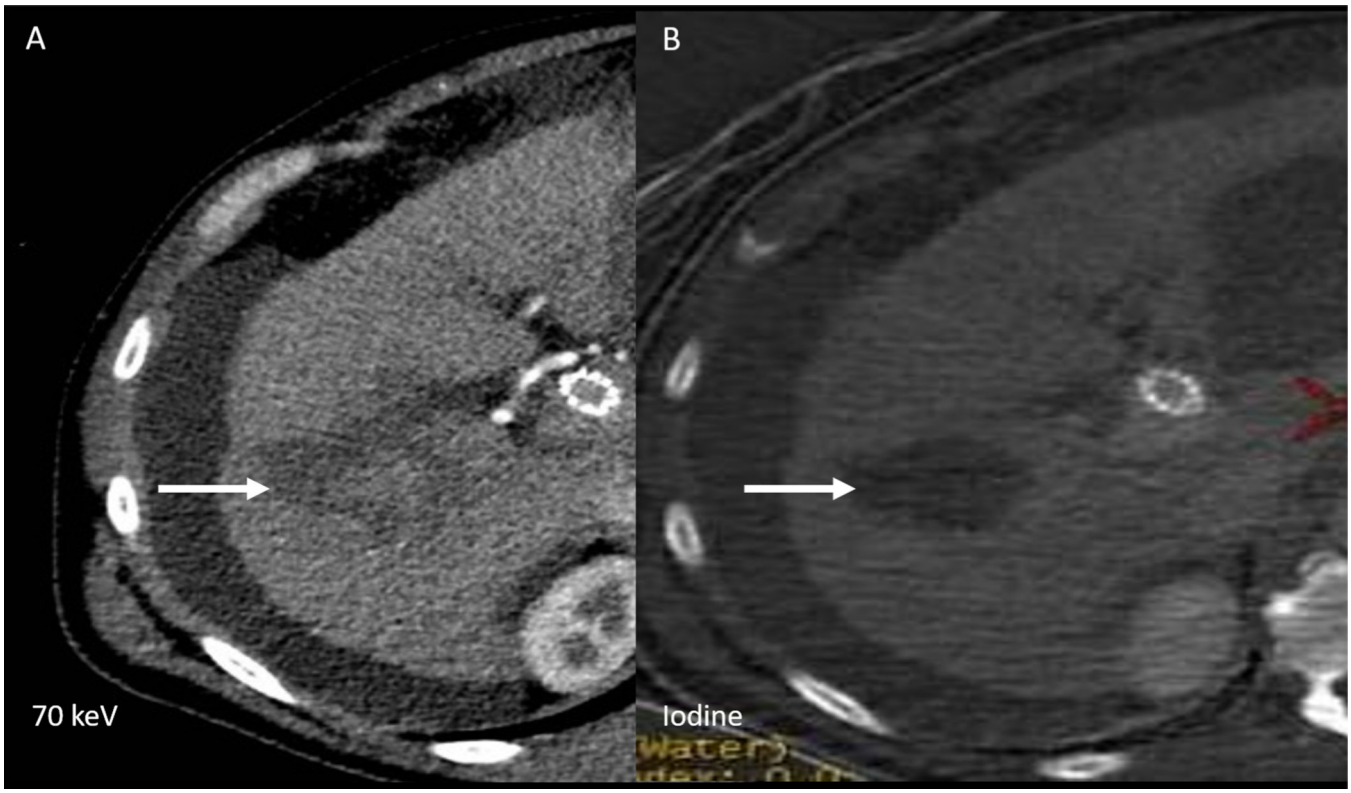

Figure 6: Therapy Monitoring following HCC Ablation.

Based on 70keV VMC image alone (A), it is difficult to differentiate between hemorrhage vs residual enhancement in the ablation bed (arrow). Iodine image (B) confirms lack of enhancement/residual disease in the ablation bed. The example highlights the benefit of iodine images in material differentiation, especially when unenhanced CT is not available for interpretation.

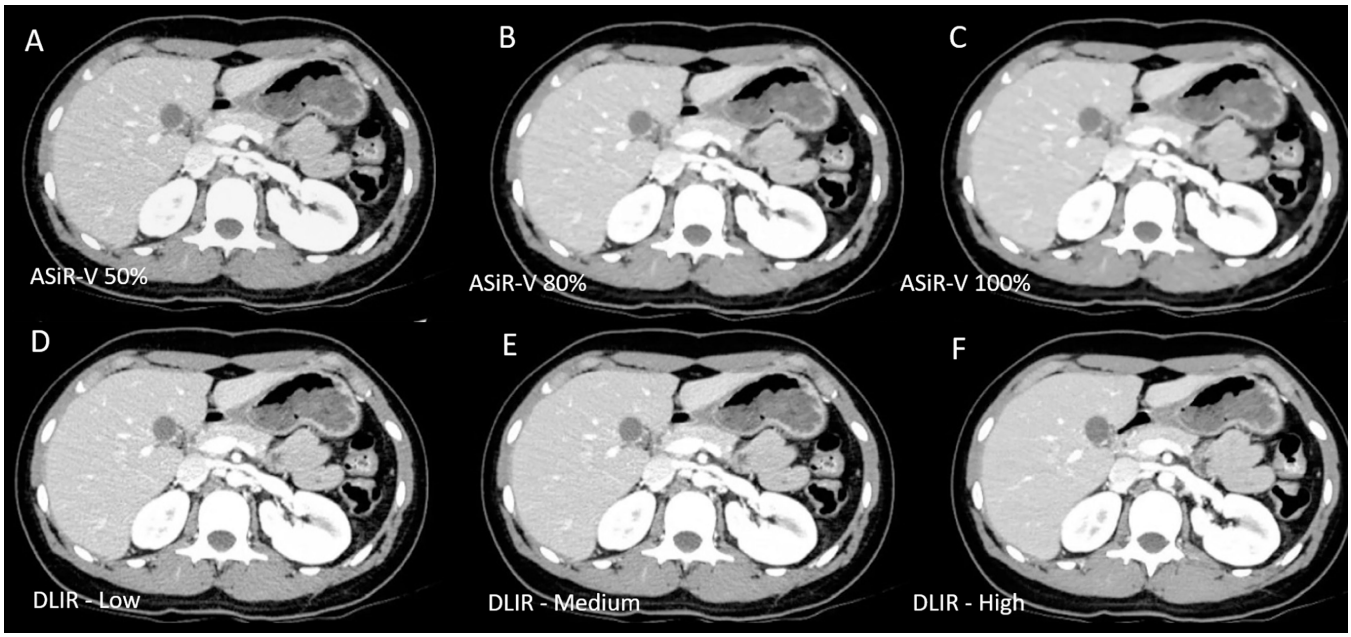

Figure 7: Deep learning image reconstruction (DLIR) for improved CT image quality.
Figure shows CT image reconstructed at different iterative reconstruction strengths (A-C) and DLIR levels (D-F). High DLIR strength image (F) has the least amount of noise and most optimal image quality. While iterative reconstruction images may reduce image noise, such images have been associated with unacceptable image texture as in (C) which was reconstructed with 100% iterative reconstruction strength. DLIR reconstructions allow for reduction in image noise with better preservation of image texture (F).

Table 1.

Basic Recommendations for Liver CT Imaging [19, 23]

Parameters	Recommendation	Rationale
CT Scanner Configuration	≥ 8-row multidetector CT	Enables rapid acquisition for multiphase imaging Enables thinner slices
Slice Thickness	2 to 5 mm	Limits volume averaging Improves detection of small lesions. Reduces noise compared to thinner slices
Multiplanar Reformats	Coronal and Sagittal planes for arterial and portal venous phases	Improves anatomical assessment. Improves lesion characterization Improves assessment for recurrence or residual disease along periphery of observations
Contrast Dose	Weight-based dosing at 1.5–2 mL/kg body weight to achieve 521–647 mg I/kg Maximum dose of 63 to 70 g Iodine in large patients	Allows for ideal maximum hepatic enhancement of at least 50 HU [20] Individualizes dosing. Maximum hepatic enhancement is inversely related to body weight. Larger patients have larger plasma and interstitial fluid volumes, diluting contrast dose [19]
Contrast Concentration	≥300 mg I/mL	Provides a reasonable volume when adjusted for appropriate contrast dose
Injection Rate	5 mL/sec if possible	Increases magnitude of arterial enhancement [23]. Increases temporal separation of arterial and portal venous phases [23]
Saline Flush	20–50 mL at same injection rate as contrast. For test bolus, use same amount and rate of saline flush as for the diagnostic bolus.	Improves contrast enhancement [23] Increases efficiency of contrast use [23].

Table 2.

Scan Delay Techniques for Capturing Late Arterial Phase [19,20,23]

Method	Advantages	Disadvantages
Fixed Scan Delay	Easiest to perform No additional radiation to determine delay	Does not account for variations in cardiac output or IV catheter issues High frequency of poorly timed late arterial phase exams in patients with non-average cardiac output or poor venous catheter placement
Bolus-Tracking	Individualizes scan delay Aims for good late arterial scan Full contrast dose used for diagnostic imaging	Additional radiation to assess target vessel density
Test-Bolus	Individualizes scan delay Aims for optimized late arterial scan Tests IV catheter integrity prior to full bolus	Least time-efficient to perform Additional radiation to assess target vessel density

Table 3.

Multiphase Liver CT Imaging and Contrast Bolus Timing [20,23]

	Scan Delay After Start of Diagnostic IV Contrast Bolus Injection		
Method	**Late Hepatic Arterial Phase**	**Portal Venous Phase**	**Delayed Phase**
Fixed Scan Delay	35–45 sec after start of injection	60–80 sec after start of injection	3–5 min after start of injection
Bolus-Tracking	Aortic threshold density: 100–150 HU Image acquisition: 10–30 sec after aortic threshold density attained	60–80 sec delay after start of injection	3–5 min after start of injection
Test-Bolus	Image acquisition: 10 to 20 seconds after peaking aortic enhancement Or Scan delay proportional to time to peak aortic enhancement (See Table 2c)	60 – 80 sec after start of injection Or Scan delay proportional to time to peak aortic enhancement (See Table 2c)	3–5 min after start of injection

Table 4.

Timing bolus scan delay look-up table [26,27].

Time to peak aortic enhancement (sec)	Late Arterial phase scan delay (sec)	Portal venous phase scan delay (sec)
6	28	60
8	30	60
10	33	60
12	36	60
13	37	62
14	39	63
15 (average patient)	**40**	**68**
16	42	71
17	43	74
18	44	78
19	46	80
20	47	84
22	50	91
24	53	97
26	56	104
28	58	110
30	61	116
32	64	122
34	67	129
36	70	136
38	72	140
40	75	147
42	78	154
44	81	161
46	84	167
48	86	172
50	89	179

Scan delays are for 5cc/sec injection, 30 mL timing bolus, 50 mL saline chase. For portal venous phase scans, add 8 seconds for 4cc/sec or 16 seconds for 3cc/sec IV contrast injections. Scan delays are based on time to peak enhancement correlations, with corrections based on IV contrast bolus durations. Timing boluses must be performed with the same injection rate and saline chase volumes as for the subsequent diagnostic contrast bolus.

Table 5

Publications on liver fat and iron quantification via DECT

Authors, Year	Cases (n)	DECT Platform and Phases Acquired	Modality Compared	DECT Method for Quantification	Reference Comparison	Liver Biopsy	Results
Studies on fat quantification[50–53]							
Zheng et al[55] (2013, retrospective)	52	SSDECT (unenhanced SECT and DECT)	Conventional unenhanced SECT (liver attenuation and liver-spleen attenuation difference/ratio)	Analysis of VMC images (1) ΔHU and spectral curve analysis (2) ROI for fat pixel on dual-energy subtraction imaging (DESI) (subtracting VMC at 75 keV from 50 keV)	Unenhanced SECT	None	Distinctive curve patterns at different grades of hepatic steatosis can be created on spectral CT. Subtraction images help in quantitative and qualitative assessment. Overall, DECT has advantages over SECT.
Patel et al[57] (20 1 3, retrospective)	363	SSDECT (unenhanced SECTand contrast-enhanced DECT)	Conventional unenhanced SECT (liver attenuation and liver-spleen attenuation difference)	Two-material decomposition algorithm fat (iodine)	Unenhanced SECT	None	Good correlation between the fat density and fat HU measurements (liver-spleen difference) on water images and SECT. A threshold of 1027 mg/mL can identify 90% of steatotic livers on contrast-enhanced DECT studied. But the study showed poor correlation between fat density measurements and the degree of steatosis.
Hyodo et al[56] (20 1 7, prospective)	33	SSDECT (contrast-enhanced DECT)	Magnetic resonance spectroscopy	Percentage of fat volume fraction from multimaterial decomposition algorithm	Magnetic resonance spectroscopy	Yes	For hepatic fat quantification on contrast-enhanced study, DECT is accurate and reproducible. This may obviate the need for the unenhanced scan.
Kramer et al[58] (20 1 7, prospective)	50	SSDECT (unenhanced DECT)	VMI (range = 70-140 keV) and material decomposition images	Unenhanced SECT, gray-scale US, US- SWE proton density fat fraction MRI	Magnetic resonance spectroscopy	None	Excellent correlation between MRS and both proton density fat fraction MRI and SECT. DECT-based material decomposition did not add value over conventional SECT in quantifying fat.
Studies on iron quantification[54-57]							
Joe et al[59] (2011, retrospective)	87	dsDECT (unenhanced DECT)	3T MRI (iron indexes calculated on T1 and T2W sequences. R2 or R2* method not used	ΔHU between 80 kVp and140 kVp	Histology	Yes	ΔHU significantly correlated with the degree of iron accumulation. At clinically important levels of LIC, DECT and MRI have similar accuracy. Δ HU of 13.8 provides specific threshold to exclude significant LIC.
Luo et al[60] (2015, prospective)	56 (MRI data from 34 patients)	dsDECT (unenhanced DECT)	1.5 T MRI (spine echo-based R2* technique)	VIC analyzed using three-material decomposition algorithm	MRI R2* technique	No	DECT-based VIC showed significant correlation with R2* and MRI- measured LIC. Diagnostic performance of DECT was similar to MRI above clinically significant iron levels.
Werner et al[62] (2019, retrospective)	110 (147 scans from	dsDECT (unenhanced DECT)	Serum ferritin and transfused iron (estimated amount)	VIC analyzed using three-material decomposition algorithm	Serum ferritin and estimated	No	DECT-based VIC algorithm strongly correlates with serum ferritin levels and estimated amount of transfused iron

Magn Reson Imaging Clin N Am. Author manuscript; available in PMC 2022 August 01.

Authors, Year	Cases (n)	DECT Platform and Phases Acquired	Modality Compared	DECT Method for Quantification	Reference Comparison	Liver Biopsy	Results
	110 patients)				amount of transfused iron		
Ma et al[61] (2020, retrospective)	31	dlDECT (unenhanced DECT)	MRI (R2* technique)	ΔHU in VMC images – between lower (50 keV) and higher (120 keV) energy levels	MRI R2* technique	No	ΔHU showed a strong linear correlation with liver R2*. The study also calculated R2* and ΔHU of cardiac muscles, but the correlation was wk.

Abbreviations: dlDECT, dual detector layer DECT; dsDECT, dual-source DECT; HU, Hounsfield units; LIC, liver iron content; MRS, MR spectroscopy; ROI, region of interest; SECT, singleenergy CT; ssDECT, single-source DECT; SWE, shear wave elastography; US, ultrasound; VIC, virtual iron content.